Ultrasensitive detection and characterisation of biomolecules using superchiral fields

E. Hendry[1], T. Carpy[2], J. Johnston[2, 3], M. Popland[2], R. Mikhaylovskiy[1], A. J. Lapthorn[2], S. M. Kelly[4], L. D. Barron[2], N. Gadegaard[3] and M. Kadodwala[2*]

[1]School of Physics, University of Exeter, Stocker Road, Exeter, EX4 4QL, UK

[2]School of Chemistry, Joseph Black Building, University of Glasgow, Glasgow G12 8QQ, UK

[3]School of Engineering, Rankine Building, University of Glasgow, Glasgow G12 8LT, UK

College of Medical, Veterinary and Life Sciences,

Institute of Molecular, Cell & Systems Biology, University of Glasgow

Glasgow G12 8QQ, UK

To whom correspondence should be addressed: malcolmk@chem.gla.ac.uk

The spectroscopic analysis of large biomolecules is important in applications such as biomedical diagnostics and pathogen detection[1,2], and spectroscopic techniques can detect such molecules at the nanogram level or lower. However, spectroscopic techniques have not been able to probe the structure of large biomolecules with similar levels of sensitivity. Here we show that superchiral electromagnetic fields[3], generated by the optical excitation of plasmonic planar chiral metamaterials[4,5], are highly sensitive probes of chiral supramolecular structure. The differences in the effective refractive indices of chiral samples exposed to left- and right-handed superchiral fields are found to be up to 10^6 times greater than that those observed in optical polarimetry measurements, thus allowing picogram quantities of adsorbed molecules to be characterised. The largest differences are observed for biomolecules that possess chiral planar

sheets, such as proteins with high β-sheet content, which suggest that this approach could form the basis for assaying technologies capable of detecting amyloid diseases and certain types of viruses.

Since the building blocks of life are chiral molecular units such as amino acids and sugars, biomacromolecules formed from these units also exhibit chirality on molecular and supramolecular scales. Chirally sensitive (chiroptical) spectroscopic techniques, such as circular dichroism (CD), optical rotatory dispersion (ORD) and Raman optical activity (ROA), are therefore especially incisive probes of the three-dimensional aspects of biomacromolecular structure and are widely used in biomolecular science [1,2]. Chiroptical methods typically measure small differences, or dissymmetries, in the interaction of left- and right-circularly polarised light, the chiral probe, with a chiral material[2]. However, the inherent weakness of these existing chiroptical phenomena usually restricts their application to samples of microgram level. Recently, Tang and Cohen[3] postulated that under certain circumstances superchiral electromagnetic fields could be produced that display greater chiral asymmetry than circularly polarised plane light waves. We have realised such superchiral electromagnetic fields are generated in the near fields of PCMs, and can greatly enhanced the sensitivity of a chiroptical measurement, enabling us to detect and characterise just a few picograms of a chiral material.

PCMs were first fabricated, and shown to display large chiroptical effects such as optical rotation, by Schwanecke and co-workers[4] and Gonokami and co-workers[5]. The PCMs used in this study, Fig. 1 (a), are composed of left or right handed (LH / RH) Au gammadions, of length 400 nm and thickness 100 nm (plus a 5 nm Cr adhesion layer) deposited on a glass substrate and arranged in a square lattice with a periodicity of 800 nm. As a control we repeated all experiments using a metamaterial composed of achiral crosses with the same thickness and periodicity as the gammadions: these structures showed no dissymmetry in excitation. Previous works on PCMs discussed their suitability as negative refractive index materials[6,7] and broadband circular polarisers[8]. Konishi *et al*[9], meanwhile, suggested that the optical excitation of the chiral localised surface plasmon resonances (LSPRs) generates chiral electric fields. For such materials the handedness of the electromagnetic field near the nanoparticle is governed by the chirality of the gammadion; reversal of the chirality of

the gammadion reverses the chirality of the generated fields. In this paper, we demonstrate for the first time the potential of utilizing chiral local fields in biosensing technologies.

UV / visible CD spectroscopy was used to probe the optical properties of the PCMs in the presence of a liquid layer (water, TRIS buffer and solutions of the chiral molecules materials). CD spectroscopy determines the *difference* in extinction spectra of the PCMs obtained with left- and right-circularly polarised light. It has the advantage over conventional UV / visible spectrometry of removing the achiral background of scattered light and achiral plasmonic resonances, considerably simplifying spectra[1]. The CD spectra from LH and RH PCMs in the presence of water are shown in Fig. 1 (a). As expected, the spectra of the LH and RH gammadions are essentially mirror images of each other: small differences in wavelengths and intensities of peaks can be attributed to variations in the level of defects between LH and RH PCMs. We observe clear resonances in the CD spectra that we attribute to the excitation of localized surface plasmons resonances (LSPRs) in the PCM structures.

A quantitative understanding of the optical properties of the PCMs can be accomplished by the application of electromagnetic modelling techniques that allow accurate simulation of the fields in the materials. Our modelling of the PCMs, Fig. 2 (a), reproduces the main features observed in the experimental CD spectra, with a slight blue shift and narrowing of the resonances (effects we attribute to rounding of edges and inhomogeneity in the experimental samples). One can clearly see the enhanced electric fields [red areas in left hand panels of Figs. 2 (b)-2 (d)] caused by coupling to LSPRs in the gold nanostructures. Molecules in these regions will undergo a much stronger interaction with the electromagnetic field than those that lie well away from metallic particles. This means that the dielectric environment of the near surface region of the gammadians will strongly influence the resonant LSPR wavelengths (λ). This phenomenon is the basis of the (bio)sensing capabilities of nanostructured plasmonic materials[10-15]. The wavelength shift ($\Delta\lambda$) of LSPR modes of nanoparticles induced by a dielectric layer is normally described approximately by Eq (1)[14, 15];

$$\Delta\lambda = m\Delta n\left[1-\exp\left(-2d/l_d\right)\right] \quad (1)$$

where m is a constant, Δn is the change in effective refractive index (from that of the buffer solution) induced by molecules near the metallic surfaces, d is the thickness of the molecular layer and l_d represents the spatial evanescent decay of local fields. The quantity, m, represents the sensitivity of the nanomaterial towards changes in local refractive index, and will be different for each LSPR mode. For the PCMs used in this study, three chiral modes, which we have labelled I, II and III, display the largest m values. These three modes display the largest $\Delta\lambda$ on changes in the local environment of the gammadions, for example on changing the refractive index of the surrounding liquid (see supplementary data).

As in previous studies[10-15], we attribute shifts in the LSPRs to adsorption of macromolecules in high field regions, which induces shifts in LSPR wavelengths. We determined how a range of adsorbed chiral materials, with different supramolecular structures, influences the chiral LSPRs. The simplest chiral adsorbate we studied is the amino acid tryptophan, which binds to the surface in a flat geometry via its carboxylate group and ring system, forming a planar "2-D" chiral monolayer[16]. We also studied six proteins: myoglobin, haemoglobin and bovine serum albumin, which have high levels of α-helical secondary structure[18], and β-lactoglobulin, outer membrane protein A (Omp A) and concanavalin A, which have high levels of β-sheet secondary structure[17]. Upon adsorption, protein tertiary structure is strongly modified by the drive to mimise the surface free energy of the interface, but secondary structure remains largely native[18].

Our data show that the supramolecular structure of an adsorbed chiral layer strongly affects the influence it has on the chiral plasmonic resonances of the PCM. This is demonstrated by the observed shifts in the resonance wavelengths ($\Delta\lambda_{LH}$ and $\Delta\lambda_{RH}$ for LSPRs of the LH and RH-PCMs, respectively) induced by adsorption of different molecular species [indicated in Fig. 1 (b)]. For the adsorption of some of the chiral molecular layers, the values of $\Delta\lambda_{LH}$ and $\Delta\lambda_{RH}$ are found to be different. We also observe a concurrent asymmetry in the LSPR intensities [note the asymmetry in the

mode III in the spectra in Fig. 1 (b)]. In contrast, for an achiral adsorption layer, no dissymmetry between LH and RH PCMs is observed (we demonstrated this by placing the PCMs in ethanol instead of water; and was further confirmed by collecting spectra from PCMs which had films of an achiral molecule deposited upon them, see supporting data). We therefore parameterised the dissymmetries in the shifts of the LSPRs on adsorption of chiral layers using $\Delta\Delta\lambda = \Delta\lambda_{RH} - \Delta\lambda_{LH}$ (see fig. 3 (b)). The largest values for $\Delta\Delta\lambda$ are found for the adsorption of tryptophan and for the three β-sheet proteins. All three β-sheet protein species induce positive values for $\Delta\Delta\lambda$, while tryptophan adsorption gives rise to negative values. The values of $\Delta\Delta\lambda$ values display a similar fingerprint for different adsorbed species; modes II and III give rise to the largest dissymmetries, while mode I displays significantly smaller dissymmetries in each case. The large dissymmetries observed for adsorption of tryptophan and the β-sheet proteins do not appear to be associated with the previously reported phenomenon of adsorbate-induced conveying of chirality onto the electronic structures of metals[19-21]; this is demonstrated by the absence of any detected optical activity from achiral crosses after the adsorption of chiral layers (see supporting data). Our observation is also unrelated to the previously reported phenomenon of CD spectra from a biomacromolecule being enhanced in the presence of a plasmonic particle[22,23]. This resonant enhancement arises because an electronic transition of the molecular system overlaps with the plasmonic resonance of the particle. The chiral materials studied have been purposely chosen so that they do not have an optical excitation that coincides with a resonance of the PCM, to preclude the possibility of observing a plasmonic resonant enhancement.

In contrast to the behaviour found for tryptophan and the three β-sheet proteins, the three α-helical proteins induce comparatively small dissymmetries ($\Delta\Delta\lambda \sim 0$ within experimental error). This behaviour cannot be attributed to lower levels, or even absence, of molecular adsorption. We verified this by monitoring the average shift $\Delta\lambda_{AV} = (\Delta\lambda_{RH} + \Delta\lambda_{LH})/2$ for the PCMs (Fig. 3 (a)), which is a measure of the thickness of the adsorbed layer. We have further confirmed adsorption levels by implementing surface plasmon resonance (SPR) measurements (supporting data). Both the SPR and $\Delta\lambda_{AV}$ data demonstrate that there is an appreciable adsorption of α-helical proteins onto the PCM surfaces. We therefore attribute the differences in the

dissymmetries exhibited by α-helical and β-sheet proteins to their distinct chiral supramolecular structures. This dependency on macromolecular structure is supported by measurements of β-lactoglobulin layers deposited onto the PCMs from solutions incubated at 70°C. Previous work has shown that β-lactoglobulin adsorbed from solution at 70ºC on to a metal surface is both aggregated and unfolded, with the loss of β-structure, while exhibiting higher levels of adsorption compared to solutions incubated at room temperature[24,25]. We observe a larger $\Delta\lambda_{AV}$ for β-lactoglobulin solutions incubated at 70°C compared to room temperature, confirming a higher adsorption of the heat treated β-lactoglobulin . A markedly smaller observed dissymmetry for heat-treated β-lactoglobulin solutions (Fig. 3 (b)) therefore demonstrates the dependence of dissymmetry on the distinct chiral supramolecular structure associated with the β-sheets.

One can evaluate the strength of the chiral interaction with the adsorbed molecular layers by estimating the dissymmetry in the effective refractive indices of the chiral layers on LH / RH-PCMs, $n_{L/R}$. Using the values for $\Delta\Delta\lambda$ from Fig. 3 (b) with Eq. 1, the following dissymmetry factor g can be determined:

$$g = \frac{n_R - n_L}{\left(n_R + n_L\right)} \tag{2}$$

The lower estimates for g obtained (see supporting data) for tryptophan and the β-sheet proteins are ~ 10^{-2} –10^{-1}. This magnitude of this dissymmetry is ~10^6 times that typically observed for the dissymmetries in the refractive indices of the chiral molecules in solution when measured by circularly polarized light (~10^{-7})[1,2].

Local field enhancement [red areas in left hand panels of Figs. 2 (b)-2 (d)] by itself is not sufficient to account for the enhanced chiral response. Due to the symmetry of the metallic structures in this case, plasmon oscillations in different branches are coupled together to generate superchiral fields. In order to parameterise the local density of chirality of an electromagnetic field, Tang and Cohen[3] introduced the following time-even pseudoscalar which they called the optical chirality:

$$C \equiv \frac{\epsilon_0}{2}\mathbf{E}\cdot\nabla\times\mathbf{E} + \frac{1}{2\mu_0}\mathbf{B}\cdot\nabla\times\mathbf{B}, \tag{3}$$

where ε_0 and μ_0 are the permittivity and permeability of free space, respectively, and **E** and **B** are the local electric and magnetic fields. When considering only dipolar excitation of molecules, the chiral asymmetry in the rate of excitation is given by the product of *C* with the inherent chiral properties of the material[3]. Tang and Cohen provided an illustration of how superchiral fields might be generated at the nodes of a standing wave, and also suggested that nanostructures may generate fields with locally enhanced chirality. In the right hand panels of Figs. 2 (b) – 2(d) we use Eq. 3 to evaluate the optical chirality of the near fields generated by our structures: the superchiral field is spatially variable, and is 1-2 orders of magnitude larger than expected for circularly polarized plane waves. The largest enhancements are clearly observed for modes II and III, while mode I exhibits very little enhancement. This observation is consistent with the larger dissymmetries observed for modes II and III in our experiments.

Chiroptical phenomena such as circular dichroism and optical rotation derive from higher order effects, the largest contributions being from electric dipole–magnetic dipole (dipolar) and electric dipole–electric quadrupole (quadrupolar) interactions, with the latter averaging to zero in isotropic media[2]. Since the definition of optical chirality given in Ref [3]is derived from dipolar excitation molecules, one can expect enhanced optical activity due to the superchiral near fields of the nanoparticles for all the chiral materials studied, including those which form isotropic overlayers on our PCM structures. However, from our electromagnetic modeling we estimate that the enhancement of dipolar chiral excitations due to superchiral fields is at most 1 to 2 orders of magnitude, and by itself cannot explain the large dissymmetries observed for tryptophan and the β-sheet proteins. We believe that the large dissymmetry enhancements observed for tryptophan and the β-sheet proteins may result from the quadrupolar contribution to optical activity. Under ordinary excitation by circularly polarized light the dipolar and quadrupolar terms can contribute to the same order of magnitude in anisotropic materials[2]. However the localchiral field around our PCM structures display steep field gradients, which will enhance, relative to the dipolar contributions, any quadrupolar contributions to optical activity. Efrima[26] has discussed the influence of the gradients of localized electromagnetic fields on the quadrupolar contribution to the optical activity displayed by an adsorbed anisotropic

chiral layer. This work showed that the level of dissymmetry factors such as *g* scale with the gradients of the localized fields. In our electromagnetic modeling (Fig. 2) we observe field gradients near our PCM structures that are three to four orders of magnitude larger than E_0/λ (the value characteristic of plane polarized light). Consequently, quadrupolar contributions to optical activity may give rise to very large dissymmetries for adsorbed anisotropic chiral media.

Upon adsorption the chiral molecules will adopt geometries in which they have an axis with a well-defined orientation with respect to the surface normal, and random orientation in the plane parallel to the surface. Due to the number and broad spatial distribution of α-helices within myoglobin, haemoglobin and BSA, in the adsorbed state they will be isotropically distributed with respect to the surface (illustrated for haemoglobin in Fig. 1 (c)). For these molecules, one therefore expects the quadrupolar contribution to the dissymmetry to be small. In contrast, the planarity of the adsorbed trypophan monolayer and β-sheet structures will result in anisotropic adsorbed layers that display C_∞ symmetry (illustrated for β-lactoglobulin in Fig. 1 (c)). The extremely large dissymmetries observed for tryptophan layers and β-sheet proteins therefore reflect the anisotropic structure of the adsorbed layers, which facilitates a large quadrupolar enhancement to the optical activity.

In conclusion the use of superchiral electromagnetic fields is a radically new approach to biospectroscopy / biosensing. The new phenomenon we describe not only allows us to detect the presence of chiral materials at the picogram level, but also to sense their structures. In the future, this will allow, *inter alia*, the monitoring of protein dynamics in ultra-small (nanofluidic) volumes, and will provide a new ultrasensitive tool for studying chiral macromolecular structure generally. The special sensitivity to β-sheet could also provide a unique capability for studying the β-structured amyloid plaques which play significant roles in diseases such as Alzheimer's, Parkinson's, and the transmissible spongiform encephalopathies. Also the phenomenon might be used to characterize minute amounts of a virus: it may be possible to discriminate rapidly between isosahedral viruses which usually have coat proteins with folds based on β-sheet, from cylindrical and filamentous viruses which usually have α-helical coat proteins folds.

Functionalisation of the PCMs would, meanwhile, allow a plethora of assay platforms to be developed (e.g. protein interactions with other macromolecules, ligands, drugs, the kinetics of fibrillization, etc).

Methods Summary

Experimental set-up

The PCMs are incorporated into a liquid cell with a pathlength of 90μm, and a total volume of 9 μL. All CD spectra were collected with a side of the PCM lattice being parallel to the laboratory frame, and with the back face (Metal / Glass) of the PCM facing the spectrometer detector (identical spectra were obtained in the reverse geometry when the front face of the PCM faced the detector). A total of ~ 3.9×10^7 gammadions were present in the optical path of the spectropolarimeter, and only these contributed to the observed spectra. CD spectra were collected using a commercial spectropolarimeter (JASCO J-810).

Solutions of chiral materials

All solutions used had a concentration of 1 mg / ml, the trytpophan solution was made up using distilled water, while the proteins solutions were made using a 10 mM Tris / HCl buffer of pH 7.4.

Cleaning Procedure

PCM substrates were used in multiple experiments. After each protein adsorption and measurement cycle, the samples were immersed in saline solution for 20 min, followed by 20 min in sodium dodectyl sulphate detergent solution, and rinsed with distilled water after each step. Finally, any remaining (organic) residue was removed in an oxygen plasma-cleaning unit (100W for 1 min).

Electromagnetic field Simulations

Numerical simulations of electromagnetic fields were performed using a commercial finite-element package (Ansoft HFSS version 11.0) with a mesh size of 4.0 nm. Permittivity values for gold were taken from E. D. Palik, *Handbook of optical constants of solids* (Academic Press, New York, 1985). The CD spectrum in Fig. 2(a) is calculated from the optical rotation of linearly polarized light according to Ref 27. The plots in Fig. 2(b-d) are calculated for excitation by LH circularly polarized light. Further details of numerical simulations can be found in the supplementary information.

Acknowledgements

We acknowledge the financial support of the EPSRC, BBSRC, Diamond light source Ltd. and the University of Glasgow (UG). We also wish to thank the technical support staff of the James Watt nanofabrication centre (UG).

Authors Contribution

M. K. conceived and designed the experiments: T. C., J. J., M. P and S. K. performed the experiments: R. M. and E. H performed numerical simulations: J. J. and N. G. fabricated the PCMs: E. H., L. D. B. and M. K. analyzed the data: A. L. and S. K. contributed materials/analysis tools: E. H., A. L., S. J., N. G. L. D. B. and M. K. co-wrote the paper.

References

1 Fasman, G.D. (ed), Circular Dichroism and Conformational Analysis of Biomolecules, Pelnum Press, 1996

2 Barron, L. D. *Molecular Light Scattering and Optical Activity*, second edition. Cambridge University Press, Cambridge, 2004

3 Tang, Y. & Cohen, A.E. Optical chirality and its interaction with matter *Phys. Rev. Lett.* **104** 163901 (2010)

4 Schwanecke, A.S. *et al*. Broken time reversal of light interaction with planar chiral nanostructures. *Phys. Rev. Lett.* **91** 247404 (2003)

5 Kuwata-Gonokami, M. *et al.* Giant optical activity in quasi-two-dimensional planar nanostructures. *Phys. Rev. Lett* **95** 227401 (2005)

6 Pendry, J.B. A chiral route to negative refraction *Science* **306** 1353-1355 (2004)

7 Zhang, S., Park, Y.S., Li, J.S., Zhang, W.L. & Zhang, X. Negative refractive index in chiral metamaterials *Phys. Rev. Lett.* **102** 023901 (2009)

8 Gansel, J.K. *et al.* Gold helix photonic metamaterial as broadband circular polariser *Science* **305** 1513 (2009)

9 Konishi, K., Sugimoto, T., Bai, B., Svirko, Y. & Kuwata-Gonokami, M. Effects of surface plasmon resonances on the optical activity of chiral metal nanogratings. *Opt. Exp.* **15** 9575-9583 (2007)

10 Willets, K.A. & van Duyne, R.P. Localised surface plasmon resonance spectroscopy and sensing. *Ann. Rev. Phys. Chem*. **58** 267-297 (2007)

11 Anker, J.N. *et al*. Biosensing with plasmonic nanosensors. *Nature Materials* **7** 442-453 (2008)

12 Hall, W.P. *et al.* Calcium-modulated plasmonic switch. *J. Am. Chem.. Soc.* **130** 5836-5837 (2008)

13 Link, S. & El-Sayed, M.A. Spectral properties and relaxation dynamics of surface plasmon electronic oscillations in gold and silver nanodots and nanorods. *J. Phys. Chem. B.* **103** 8410-8426 (1999)

14 Haes, A.J. & van Duyne, R.P. A nanoscale optical biosensor: Sensitivity and selectivity of an approach based on the loacalised surface plasmon resonance spectroscopy of triangular silver nanoparticles. *J. Am. Chem. Soc.* **124** 10596-10604 (2002)

15 Jung, L.S., Campbell, C.T., Chinowsky, T.M., Mar, M.N. & Yee, S.S. Quantitative interpretation of the response of surface plasmon resonance sensors to adsorbed film. *Langmuir* **14** 5636-5648 (1998)

16 Zhao, X., Zhao, R.G. & Yang, W.S. Self-assembly of L-trytophan on the Cu(001) surface. *Langmuir* **18** 433-438 (2002)

17 Berman, H.M, Henrick, K.& Nakamura, H. Announcing the worldwide protein data bank. *Nat. Struct. Biol.* **10** 980-980 (2003)

18 Malmsten, M., Chapter 1 (2000) "Protein Architecture: Interfacing Molecular Assemblies and Immobilization Biotechnology." Marcel Dekker New York

19 Mulligan A. *et al.* Going beyond the physical: Instilling chirality onto the electronic structure of a metal *Ange. Chem. Int. Ed.* **44** 1830-1833 (2005)

20 Bovet, N., McMillan, N., Gadegaard, N. & Kadodwala, M. Supramolecular assembly facilitating adsorbate-induced chiral electronic states. *J. Phys. Chem B,* **11** 10005 10011 (2007)

21 Gautier, C. & Burgi, T. Chiral N-isobutyryl-cysteine protected gold nanoparticles: Preparation, size selection, and optical activity in the UV-vis and infrared. *J. Am. Chem. Soc.* **128** 11079-11087 (2006)

22 Lieberman, I., Shemer, G., Fried, T., Kosower, E.M. & Markovich, G. Plasmon-Resonance-Enhanced Absorption and Circular Dichroism. *Ange. Chem. Int. Ed.* **47** 4833-4857 (2008)

23 Baev, A., Samoc, M., Prasad, P.N., Krykunov, M. & Autschbach, J. A quantum chemical approach to the design of chiral negative index materials. *Opt. Exp.* **15** 5730-5741 (2007)

24 Arnebrant, T., Barton, K. & Nylander, T. Adsorption of α-lactalbumin and β-lactoglobulin on metal surfaces versus temperature. *J. Coll. Int. Sci.* **119** 383-390 (1987)

25 Eloffsson, U.M., Paulsson, M.A., Sellers, P. & Arnebrant, T. Adsorption during heat treatment related to the thermal unfolding aggregation of β-lactoglobulin A and B. *J. Coll. Int. Sci.* **183** 408-415 (1996)

26 Efrima, A. Raman optical activity of molecules adsorbed on metal surfaces: Theory. *J. Chem. Phys.* **83** 1356-1362 (1985)

27 Cantor, C.R.& Schimmel P.R., *Biophysical Chemistry*, Vol.2, Chapter 8 (1980

Figures:

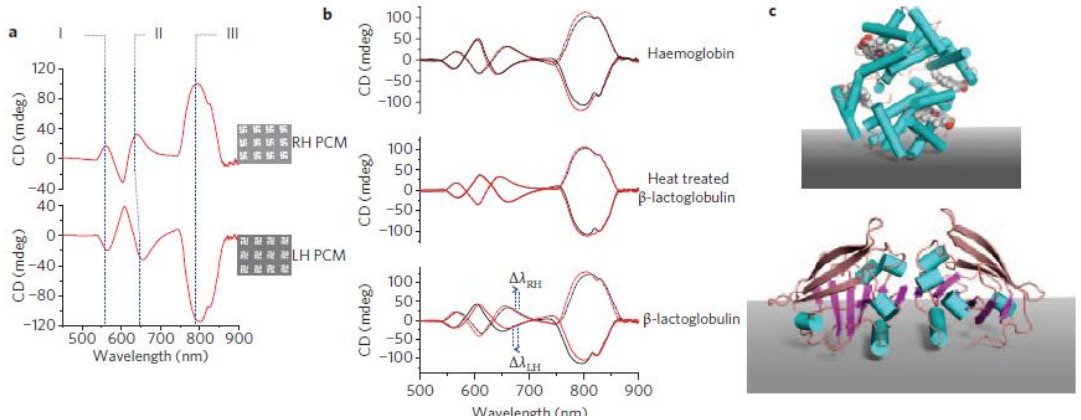

Fig. 1 Changes induced in the chiral plasmonic resonances of the PCM are readily detected using CD spectroscopy **(a)**. CD spectra collected from LH / RH-PCMs immersed in distilled water. The three modes which show the largest sensitivity to changes in the local refractive index of the surrounding medium have been labelled I , II and III. Shown to the right of each spectrum is an electron micrograph of the PCM displaying the gammadion structure and periodicity. **(b)** The influence of the adsorbed proteins haemoglobin, β-lactoglobulin, and thermally denatured β-lactoglobulin on the CD spectra of the PCMs. The red spectra were collected in Tris buffer prior to protein adsorption (solid line LH-PCM, dashed line RH-PCM) and the black were collected after protein adsorption. The magnitudes and directions of $\Delta\lambda_{RH\,/\,LH}$ values of mode II for β-lactoglobulin adsorption have been highlighed. **(c)** Haemoglobin (upper) and β-lactoglobulin (lower) are shown [α-helix (cyan cylinder) and β-sheet (ribbons)], adopting a well defined arbitary structure with respect to a surface. The figure illustrates the more anisotropic nature of adsorbed β-lactoglobulin.

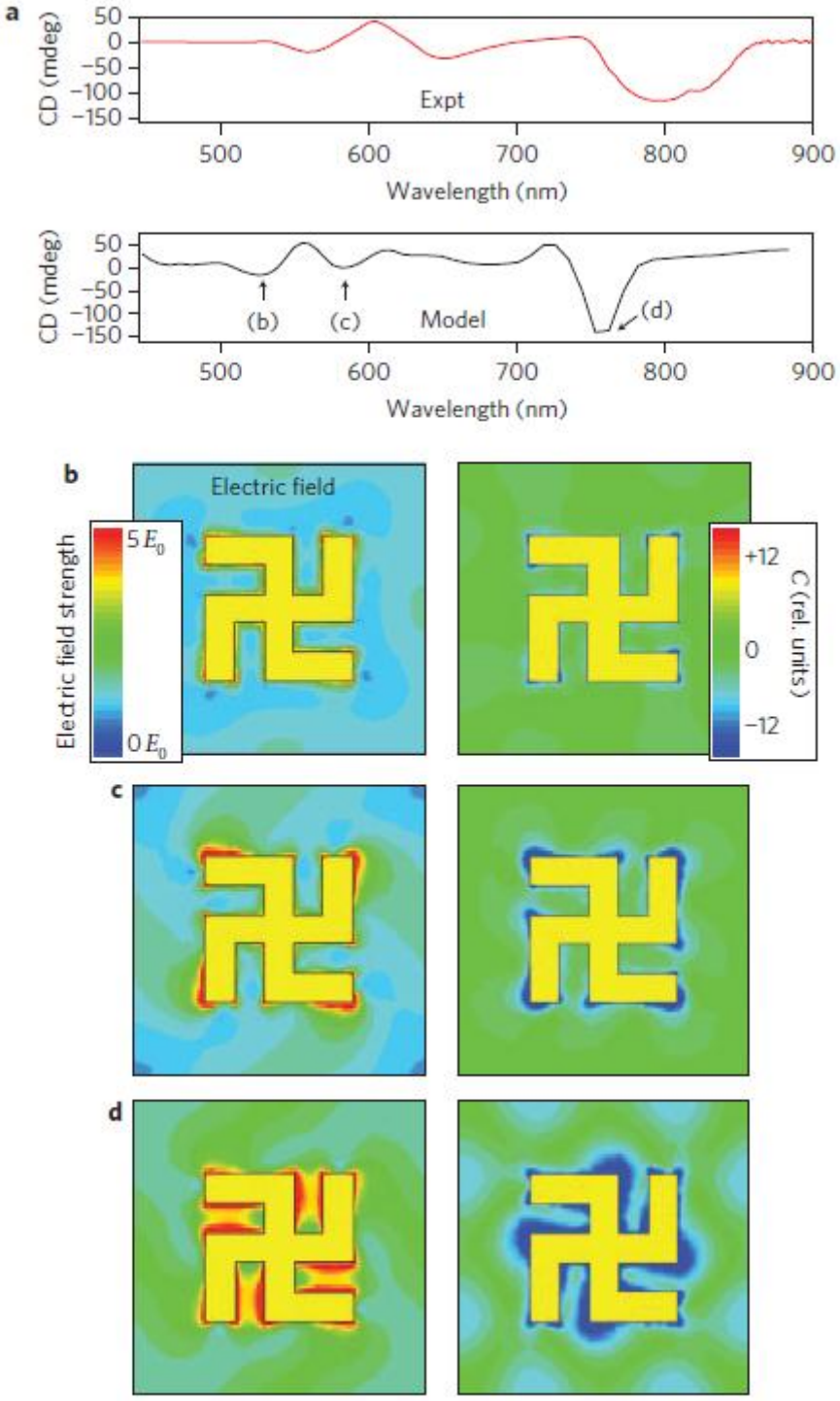

Fig. 2 Finite element modelling of the local electromagnetic fields around our PCMs. **(a)** Comparison between experimental and modelled CD spectra. **(b, c, d)** Left hand panels: Time averaged electric field strength at the wavelength marked by arrows in **(a)**, when excited by LH circularly polarized light. All fields are calculated at the substrate interface of the sample and normalized by the incident electric field (E_0). Right hand panels: Local optical chirality, *C*, as defined in equation 3, normalized by the magnitudes for LH circularly polarized plane waves.

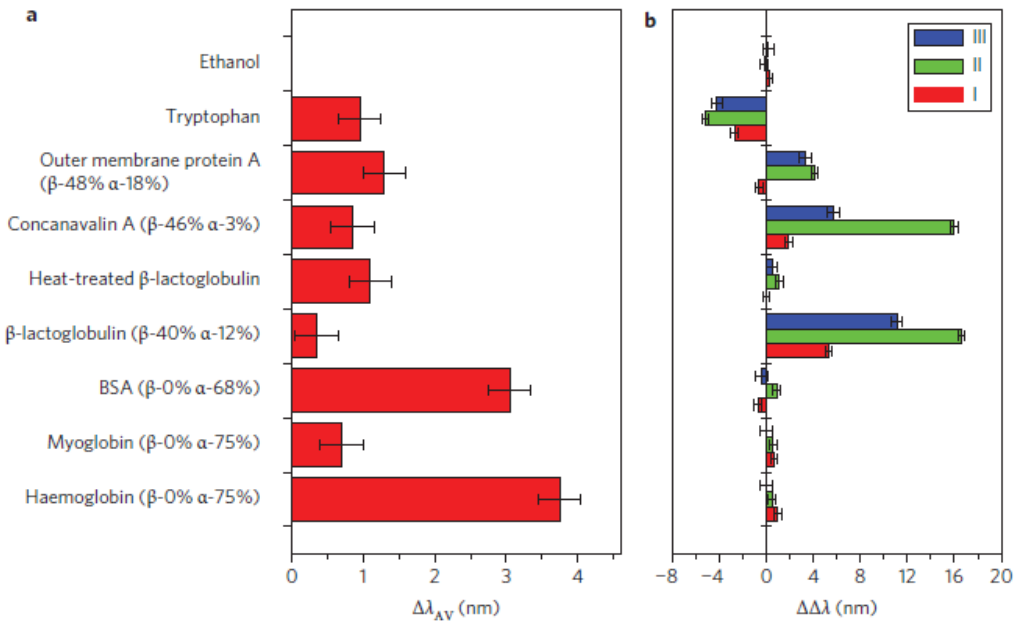

Fig.3 Values of $\Delta\Delta\lambda$ and $\Delta\lambda_{AV}$ induced by the adsorption of the chiral materials. **(a)** A plot of $\Delta\lambda_{AV}$ (TM) for tryptophan and the six proteins. **(b)** The corresponding $\Delta\Delta\lambda$ values for TM,II and III modes are displayed. Also shown are the effectively zero $\Delta\Delta\lambda$ values obtained from the (achiral) ethanol solvent.